materials

MDPI

Article

Mathematical Models of Grinding Forces in the Hob Cutter Sharpening Process

Błażej Witkowski, Wojciech Stachurski, Witold Pawłowski, Małgorzata Sikora and Norbert Kępczak *

Institute of Machine Tools and Production Engineering, Faculty of Mechanical Engineering, Lodz University of Technology, Stefanowskiego 1/15, 90-537 Lodz, Poland; blazej.witkowski@p.lodz.pl (B.W.); wojciech.stachurski@p.lodz.pl (W.S.); witold.pawlowski@p.lodz.pl (W.P.); malgorzata.sikora@p.lodz.pl (M.S.)
* Correspondence: norbert.kepczak@p.lodz.pl

Abstract: The article presents the results of research aimed at developing mathematical models for determining the components of grinding force occurring during the sharpening of the rake face of hob cutters. The development of the models was based on the results obtained during experimental tests conducted in the first stage of the research. The studies were carried out using a tool grinder and an aluminum oxide grinding wheel. During the tests, two components of the grinding force were measured, using a piezoelectric dynamometer. A sample made of HS6-5-2 high-speed steel was ground. Grinding was carried out using different sets of cutting parameters. Based on the obtained measurement results, two mathematical models were developed in the form of (1) a multiple regression function and (2) a polynomial function, enabling the calculation of the normal and the tangential force. The experimentally obtained results were then compared with those calculated based on the developed models, and the results of this comparison showed that the developed models provide a good basis for analyzing the sharpening process of hob cutters in terms of variable grinding parameters.

Keywords: grinding; hob cutter; sharpening of cutting tools; grinding force; modelling of grinding force

check for updates

Academic Editor: Zhenyu Zhang

Received: 8 December 2024
Revised: 30 December 2024
Accepted: 30 December 2024
Published: 1 January 2025

Citation: Witkowski, B.; Stachurski, W.; Pawłowski, W.; Sikora, M.; Kępczak, N. Mathematical Models of Grinding Forces in the Hob Cutter Sharpening Process. *Materials* **2025**, *18*, 138. https://doi.org/10.3390/ma18010138

Copyright: © 2025 by the authors. Licensee MDPI, Basel, Switzerland. This article is an open access article distributed under the terms and conditions of the Creative Commons Attribution (CC BY) license (https://creativecommons.org/licenses/by/4.0/).

1. Introduction

In the era of mass industrial production of gears [1], the proper regeneration of hob cutters, cutting tools commonly used for manufacturing toothed elements, is of great importance [2]. This is because improperly selected grinding conditions during the sharpening of the rake surfaces of the cutters can adversely affect the technological properties of the surface layer, causing, among other things, high thermal stresses leading to a network of cracks [3,4], and structural changes significantly reducing the cutting properties of the edges [5] and deteriorating their operational properties [6].

Therefore, it is extremely important to consciously shape the surface layer during grinding. The means to achieve this is to assess the course of the machining process, and one of the most important elements allowing for such an assessment is the knowledge of cutting forces. The significance of such an assessment lies in the dependence of the adjustable machining values, such as grinding parameters, the geometry of the contact between the grinding wheel and the workpiece, the characteristics of the grinding wheel, and the material properties on the values of the occurring forces. Moreover, knowledge of the obtained values of the grinding force components allows, among other things, for the determination of the grinding force coefficient μ, which provides information about the grinding efficiency [7], and the calculation of the total grinding power P, enabling the

determination of the grinding index K_s [8]. Generally, the grinding force is considered a key indicator of the material removal process, which directly affects the machining efficiency, the quality of the machined surface, and the durability of the grinding wheel [9].

In a broader perspective, the values of the grinding force components obtained experimentally allow for the creation of mathematical models, and the force model is the simplest and most versatile mathematical expression describing the mechanical behaviour of material removal [9]. As shown by the comparative analysis presented in the study [9], mathematical models of the grinding force can come from various sources, including experimental data, empirical formulas, or theoretical analyses. It should be remembered that modelling the grinding force is a complex process, and the factors influencing the magnitude of the grinding force can include the physical properties of the machined material, the shape, size, and number of abrasive grains, grinding parameters, cooling and lubrication conditions, and the type of grinding process [10–12].

It is worth noting that grinding force models can be used in further research to model the dynamic grinding process. An example of such use is the model of the external plunge grinding process [13–15], the process of longitudinal cylindrical external grinding [16], and the process of peripheral surface grinding [17].

Therefore, this article presents research work, as a result of which two mathematical models were determined to predict the components of the grinding force during the sharpening of the rake surfaces of hob cutters. The research began with experimental studies, the conditions and methodology of which, as well as the results, are described in Sections 2 and 3, respectively. The first of the two mathematical models presented in Section 4 is a modification of the model proposed by Werner [18]. It is worth noting that this model is often used, also with appropriate modifications, by other researchers [12,19,20]. The second mathematical model in the form of a multiple regression function was determined on the basis of algorithm of the "acceptance and rejection" method [21]. In the final part of the work, a comparison of the results obtained based on calculations using the proposed mathematical models with the results obtained experimentally was made. The work concludes with a summary and conclusions.

2. The Conditions and Methodology of the Research

The experimental studies were conducted on the ASP-631 F-SL tool grinder (Lakfam, Kowary, Poland), a general view of which is shown in Figure 1. The ASP-631 F-SL is a numerically controlled grinder in three axes for the automatic grinding of cutting tools along straight and helical lines. As such, it can be used for sharpening the rake surfaces of hob cutters.

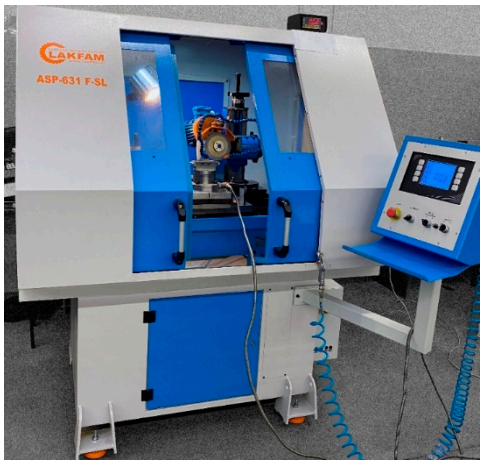


Figure 1. A general view of the ASP-631 F-SL tool grinder (Lakfam, Kowary, Poland).

In Figure 2, the workspace of the ASP-631 F-SL tool grinder is shown. As can be observed, a 4-component piezoelectric dynamometer type 9272 (Kistler, Winterthur, Switzerland) is mounted on the grinder table, previously separated from the table by a layer of insulator. The dynamometer was used to measure the components of the grinding force—the normal component F_n and the tangential component F_t. The signal from the dynamometer was transmitted to a four-channel amplifier Kistler type 5019A, then to the data acquisition card type KUSB-3108 (Keithley Instruments, Cleveland, OH, USA), which was finally connected to a PC. The Keithley quick DAQ software (version 1.6) was used to record the measurement signal.

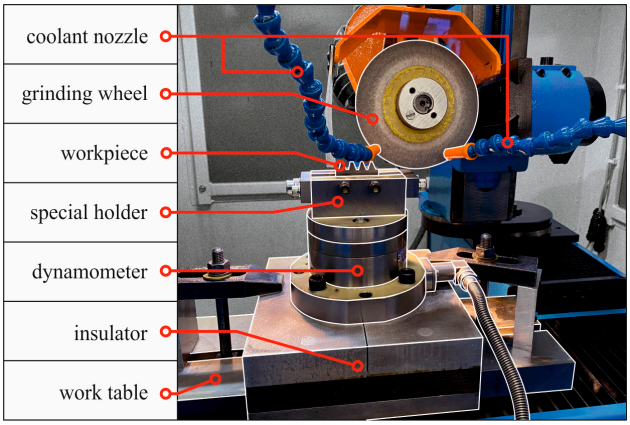


Figure 2. A view of the workspace of the ASP-631 F-SL tool grinder.

A special holder for mounting the sample was attached to the upper surface of the dynamometer. During the tests, a sample made of high-speed steel HS6-5-2 with a hardness of 62 ± 1 HRC was ground. The shape of the sample in the part subjected to grinding had the outline of a gear, with dimensions corresponding to the dimensions of the cutting edge gear of a hob cutter with a module m = 3 mm and a pressure angle $\alpha = 20^{\circ}$, in accordance with ISO 53 and ISO 54. The geometric dimensions of the gear were selected according to PN 4468, taking into account the accuracy of the hob cutter edge in class B.

As the cutting tool, a T3 type grinding wheel with dimensions ($D \times T \times H$) 125 × 9/2 × 32 mm was used. The parameter D denotes the outer diameter of the grinding wheel, the parameter T is its thickness, and the parameter H specifies the diameter of the central hole. It is worth noting that due to the conical shape of the grinding wheel's active surface, the thickness T varies from 2 mm to 9 mm. The grinding wheels were made of alumina with a vitrified bond and marked with the symbol 38A60KVBE (Norton, Koło, Poland).

During the tests, a constant grinding speed v_s, six workpiece speeds v_w, and three cutting depths a_e were used, allowing for 18 sets of cutting parameters. The machining conditions used during the tests are summarized in Table 1.

Each grinding test began with 10 spark-out passes. Then, a grinding test was carried out by removing the machining allowance (depth of cut) a_e in one work cycle consisting of two passes: a working (grinding) pass and a return pass. The working pass was performed in the counter-direction, while the return pass was performed in the co-direction, without disengagement.

During the entire grinding test, the signal from the dynamometer was recorded using the previously discussed measurement setup. As mentioned earlier, two components of the grinding force were recorded—the normal component F_n and the tangential component F_t (Figure 3). The component F_n is the force acting perpendicular to the ground surface, while the component F_t is the force acting parallel to that surface.

Table 1. Grinding conditions used during experimental tests.

Workpiece material	HS6-5-2, carburized and hardened with 62 ± 1 HRC
Grinding wheel	38A60KVBE
Grinding wheel rotational speed	n_s = 4600 rpm
Grinding wheel peripheral speed	v_s = 30.1 m/s
Workpiece speed	v_{w1} = 0.9 m/min v_{w2} = 1.0 m/min v_{w3} = 1.2 m/min v_{w4} = 1.3 m/min v_{w5} = 1.5 m/min v_{w6} = 1.6 m/min
Machining allowance (working engagement, grinding depth)	a_{e1} = 0.01 mm a_{e2} = 0.02 mm a_{e3} = 0.03 mm
Number of passes: grinding/return	1/1
Grinding direction	Up grinding
Dresser	Single-point diamond dresser
Dresser weight	Q_d = 1.0 kt (0.2 g)
Grinding wheel peripheral speed while dressing	v_{sd} = 30.1 m/s
Dressing allowance	a_d = 0.01 mm
Axial table feed speed while dressing	v_{fd} = 40 mm/min
Number of dressing passes	i_d = 10
Environments	WET—conventional flood method
Coolant	AGIP Aquamet 104 Plus in a 5% concentration
Coolant flow rate	Q = 3 L/min

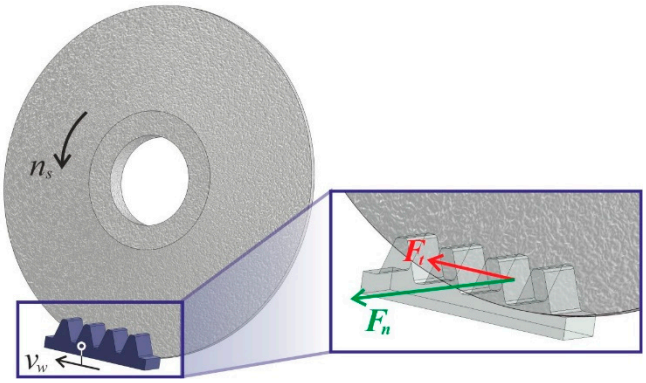


Figure 3. Distribution of grinding force components: F_t—tangential component; F_n—normal component; n_s—grinding wheel rotational speed; v_w—workpiece speed.

As the cooling and lubricating fluid, a water–oil emulsion based on AGIP Aquamet 104 Plus oil in 5% concentration was used. Aquamet 104 Plus is a semi-synthetic emulsifying oil containing mineral and synthetic oils, as well as anticorrosive, detergent, and EP additives. The oil manufacturer states that its kinematic viscosity (at 40 °C) ν = 28 mm^2/s, and its density (at 20 °C) ρ = 1.01 g/cm^3. Emulsion was supplied to the grinding zone through two nozzles with a total flow rate of Q = 3 L/min.

3. Experimental Results

In Figure 4, an example time plot of the tangential component F_t and the normal component F_n of the grinding force is presented, recorded during the working pass using the following machining parameters: a_e = 0.01 mm and v_w = 0.9 m/min.

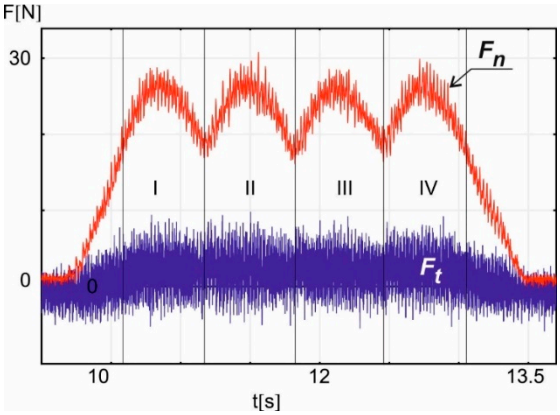


Figure 4. A sample time course of the tangential component F_t and the normal component F_n of the grinding force during the working pass; a_e = 0.01 mm, v_w = 0.9 m/min, sampling frequency 10 kHz.

As shown in the above graph, the shape of the course of both components of the grinding force depends on the length of contact between the grinding wheel and the workpiece. This length changes with the position of the grinding wheel relative to the gear-shaped sample with four teeth. For this reason, the graph is divided into four segments of force variability, corresponding to the four teeth of the hob cutter edge. These segments are numbered sequentially as I, II, III, and IV.

As can be observed in Figure 4, the highest value of the grinding normal force components in each of the four segments was obtained near the tooth tips, where the contact line is the longest. Similarly, the lowest value of the grinding force components was recorded at the tooth roots, where the contact line is the shortest.

It is worth noting that the presented force measurement is noisy. Fourier transformation showed that the noise frequency is close to the frequency associated with the variable dimensions of the gear-shaped sample.

The example time plot of the grinding force components shown in Figure 4 was obtained for one of the 54 measurements conducted under different machining conditions, considering three repetitions for each of the 18 sets of grinding parameters. To quantitatively compare the obtained results, the average value of F_t and F_n from segment II was calculated for each of the 54 working passes. This segment was taken from the full measurement, from the moment of reaching the minimum near segments I and II, to reaching the next minimum near segments II and III, as shown in Figure 4. Then, each of the three calculated average values for each of the 18 sets of grinding parameters was used to determine the average value of F_t and F_n representing a specific set of grinding parameters.

In Figure 5, the average normal component F_n of the grinding force is shown as a function of the workpiece speed v_w and three different values of machining allowance a_e. The smallest and largest values for each of the 18 sets of measurement results are also marked on the graph.

Similarly to the above, Figure 6 shows the average tangential component F_t of the grinding force as a function of the workpiece speed v_w.

As shown in Figures 5 and 6, increasing the workpiece speed v_w at a constant grinding depth ae causes an increase in both the normal component F_n and the tangential component F_t of the grinding force. A similar effect is observed when increasing the grinding depth a_e while maintaining a constant workpiece speed v_w, as shown in Figures 7 and 8. As expected, the smallest values of both F_n and F_t were achieved during grinding at the lowest workpiece speed (v_w = 0.9 m/min), while simultaneously removing the smallest machining allowance (a_e = 0.01 mm).

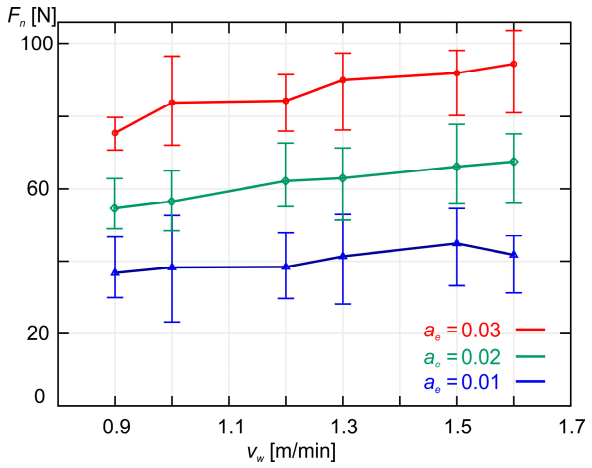


Figure 5. A plot of the average values of the normal component F_n of the grinding force as a function of the workpiece speed v_w for three different values of machining allowance a_e.

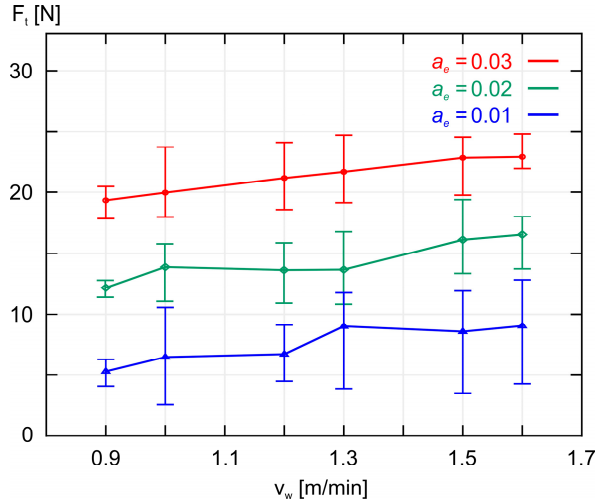


Figure 6. A plot of the average values of the tangential component F_t of the grinding force as a function of the workpiece speed v_w for three different values of machining allowance a_e.

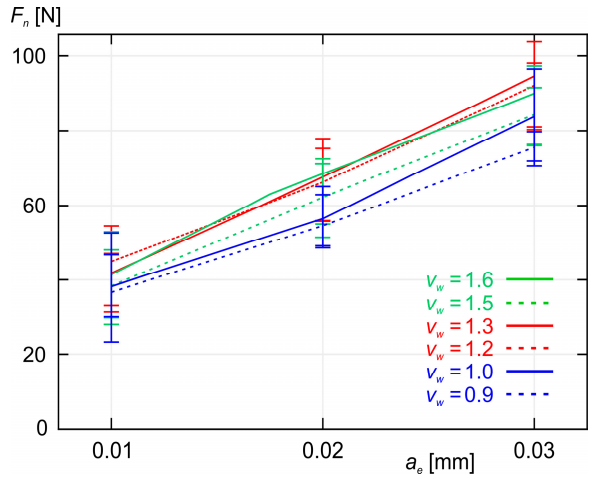


Figure 7. A plot of the average values of the normal component F_n of the grinding force as a function of the machining allowance a_e for six different values of workpiece speed v_w.

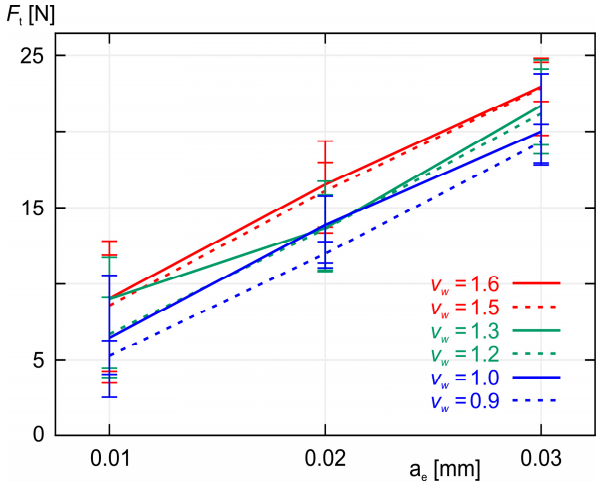


Figure 8. A plot of the average values of the tangential component F_t of the grinding force as a function of the machining allowance a_e for six different values of workpiece speed v_w.

4. Force Models of Grinding Process

4.1. The Polynominal Model Force

The obtained experimental results allowed for the construction of a model for the normal component and the tangential component of the grinding force occurring during the hob cutter sharpening process. The models for the normal component F_n available in the literature gave divergent results compared to the conducted experiment. Ultimately, the best-fitting model was accepted, whose general form as a polynomial for the normal component F_n was presented by Werner in [18]:

$$F_n = K \cdot [C_1]^{\gamma} \cdot \left[\frac{Q'_w}{v_s}\right]^{2\in-1} \cdot [a_e]^{1-\in} \cdot [d_s]^{1-\in}, \quad (1)$$

where K is the proportionality factor, C_1 is the cutting edge density, γ is an exponent depending on the grinding parameter, Q'_w is the specific material removal rate, v_s is the grinding wheel peripheral speed, $\in$ is an exponent depending on the workpiece material, a_e is a grinding depth, and d_s is the diameter of the grinding wheel.

Based on Equation (1), our own mathematical model was proposed, encompassing both components of the grinding force, in the form of the equation:

$$F_{n,t}(v_w, a_e) = K \cdot \left(\frac{v_w}{v_s}\right)^{2f-1} \cdot \left(\frac{a_e}{D}\right)^{f} \cdot D, \quad (2)$$

where

K—grinding coefficient, N/mm;
f—exponential coefficient;
v_w—workpiece speed, m/min;
v_s—grinding wheel peripheral speed, m/s;
a_e—grinding depth, mm;
D—grinding wheel outer diameter, mm.

Based on the results obtained from the experimental studies, the parameters of the mathematical model were calculated using the least squares method, in the Mathematica software (version 8). After substituting them into Equation (2), two equations for calculating the components of the grinding force were obtained:

$$F_n(v_w, a_e) = 506.751 \cdot \left(\frac{v_w}{v_s}\right)^{0.3622} \cdot \left(\frac{a_e}{D}\right)^{0.6811} \cdot D, \quad (3)$$

$$F_t(v_w, a_e) = 598.263 \cdot \left(\frac{v_w}{v_s}\right)^{0.5995} \cdot \left(\frac{a_e}{D}\right)^{0.7998} \cdot D, \quad (4)$$

where

v_s = 30.1 m/s;
D = 125 mm.

The multiple regression coefficient for these procedures was estimated at 0.9989 for normal force F_n and 0.9946 for tangential force F_t.

4.2. The Regression Analysis Procedure

To determine the mathematical relationships for calculating the normal component F_n and the tangential component F_t of the grinding force, the SKZ program (version 1.0) was used, which has been successfully developed and utilized by the authors in other research works [22–24]. The measured values from the experimental studies were used as input data.

The SKZ program determines the coefficients of the multiple regression equation using a regression analysis procedure based on the "acceptance and rejection" method [21]. The selection of critical values of the statistic (F_{kr}) is made at a significance level of α = 0.4, and after determining the regression function, it is changed to a value of α = 0.1. Calculations begin with the simplest regression function, sequentially adding new terms. When a newly added term reduces the significance of an already introduced term, it is considered insignificant and removed from the regression function. After introducing all significant terms, a panel with a preview of the calculation results is displayed on the monitor screen.

Ultimately, the function of the research object took the following general form:

$$F_{n,t} = F_0 \cdot (v_w)^{f_v} \cdot (a_e)^{f_a}, \quad (5)$$

where

F_0—constant of the equation;
f_v, f_a—exponents of the equation.

The constants and coefficients determined from the calculations allowed for obtaining the relationship for the normal component F_n of the grinding force with a multiple correlation coefficient R = 0.8893:

$$F_n = 876.6 \cdot (v_w)^{0.338} \cdot (a_e)^{0.685}. \quad (6)$$

Similar calculations allowed for obtaining the relationship for the tangential component F_t of the grinding force with a multiple correlation coefficient R = 0.8604:

$$F_t = 775.9 \cdot (v_w)^{0.529} \cdot (a_e)^{1.052}. \quad (7)$$

The significance of the obtained multiple correlation coefficients R was determined using the Fisher–Snedecor F-test. For this purpose, the test values of the F factor were calculated and compared with the critical values F_{kr}. Since the F values are greater than the F_{kr} values, the correlation coefficients should be considered significant, which, as indicated in [25], entails the agreement (at a significance level of α = 0.1) of the regression function equation with the results of the conducted experimental studies.

4.3. Comparison of Models and Experiment Results

Despite the satisfactory values of the multiple correlation coefficients for the developed mathematical models, they were also verified by comparing the calculated values of the normal component F_n and the tangential component F_t of the grinding force with the values obtained during the experimental studies. For this purpose, the values of the grinding force components F_n and F_t were calculated for the 18 sets of grinding parameters used in the studies using Equations (6) and (7). Additionally, the values of both force components were also determined based on Equations (3) and (4) of the polynomial model.

In Figure 9, a comparison of the experimental results with the results obtained from the mathematical models describing the normal component F_n of the grinding force is presented. A similar graph showing the tangential component F_t of the grinding force is shown in Figure 10.

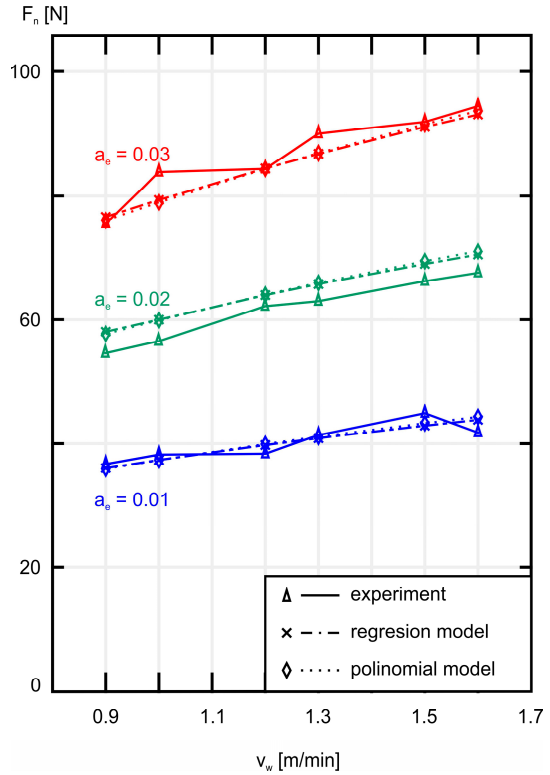


Figure 9. A plot of the experimental (solid line), regression model (point line), and polynomial model (dotted line) values of mean normal forces F_n versus workpiece speed v_w for three grinding depths a_e.

The calculation results of F_n and F_t obtained from the two presented models are summarized in Tables 2 and 3, respectively. In the case of the normal component F_n of the grinding force, the relative errors of the models are larger compared to those obtained for the tangential component F_t of the grinding force. The largest relative error for F_n in the regression model occurs at a grinding depth a_e = 0.01 mm ($\overline{|\Delta|}$) = 3.820%), while for the polynomial model it occurs at a grinding depth a_e = 0.02 mm ($\overline{|\Delta|}$) = 3.922%). Nevertheless, the overall average errors for both models remain relatively small, amounting to 3.241% for the regression model and 3.228% for the polynomial model.

It is worth noting that the largest relative error for the models of the tangential component F_t of the grinding force is observed in the regression model ($\overline{|\Delta|}$) = 2.016%) and the polynomial model ($\overline{|\Delta|}$) = 2.755%) at the same grinding depth a_e = 0.01 mm, which is the smallest. The overall average error for both models is quite small, amounting to 1.409% for the regression model and 1.727% for the polynomial model.

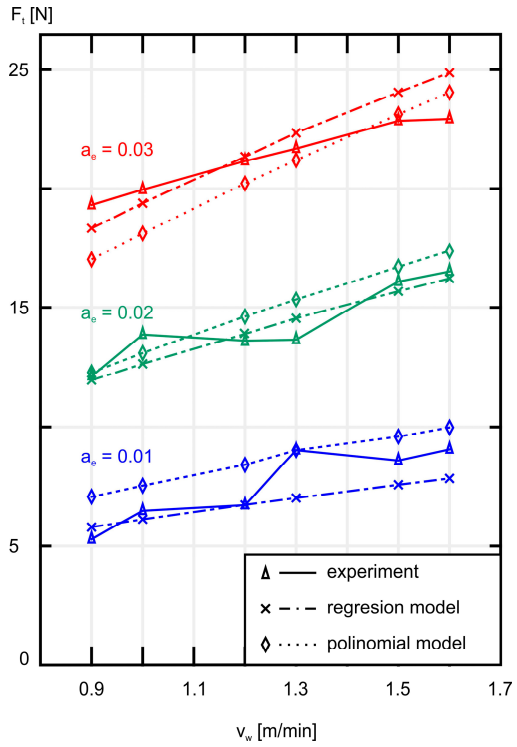


Figure 10. A plot of the experimental (solid line), regression model (point line), and polynomial model (dotted line) values of mean tangential forces F_t versus workpiece speed v_w for three grinding depths a_e.

Analyzing Tables 2 and 3, as well as Figures 9 and 10, it can be seen that both models effectively replicate the experimental results. In the case of the normal component F_n, the results obtained from both models are almost identical, while for the tangential component F_t, the results show a very small relative error despite the irregular course of the experimental results. Therefore, the results calculated based on the presented models and the results obtained from the experiment are consistent with each other.

Table 2. The values of the normal component F_n of the grinding force obtained experimentally and calculated based on models.

Input Data			**Regression Model**					**Polynomial Model**				
v_w **[m/min]**	a_e **[mm]**	**Normal Force F_n [N] (Experiment)**	**Normal Force F_n [N] (Regression Model)**	**Error $\lvert\Delta\rvert$**	**Percentage Error $\frac{\lvert\Delta\rvert}{F_t}\cdot 100\%$**	**Average Error $\sum\frac{\lvert\Delta_i\rvert}{n}$**	**Percentage Average Error $\sum\frac{\lvert\Delta_i\rvert}{F_t n}*100\%$**	**Normal Force F_n [N] (Polynomial Model)**	**Error $\lvert\Delta\rvert$**	**Percentage Error $\frac{\lvert\Delta\rvert}{F_t}\cdot 100\%$**	**Average Error $\sum\frac{\lvert\Delta_i\rvert}{n}$**	**Percentage Average Error $\sum\frac{\lvert\Delta_i\rvert}{F_t n}*100\%$**
0.9	0.01	37.799	36.086	1.713	4.533	1.597	3.820	35.968	1.831	4.844	1.620	3.896
1.0		39.294	37.394	1.900	4.835			37.367	1.927	4.903		
1.2		39.438	39.771	0.333	0.844			39.918	0.480	1.218		
1.3		42.405	40.862	1.543	3.640			41.092	1.313	3.095		
1.5		45.966	42.886	3.080	6.700			43.278	2.688	5.847		
1.6		42.817	43.832	1.015	2.371			44.302	1.485	3.468		

Table 2. *Cont.*

Input Data		Regression Model						Polynomial Model				
v_w [m/min]	a_e [mm]	Normal Force F_n [N] (Experiment)	Normal Force F_n [N] (Regression Model)	Error $\lvert\Delta\rvert$	Percentage Error $\frac{\lvert\Delta\rvert}{F_t}\cdot 100\%$	Average Error $\sum\frac{\lvert\Delta_i\rvert}{n}$	Percentage Average Error $\sum\frac{\lvert\Delta_i\rvert}{F_t n}*100\%$	Normal Force F_n [N] (Polynomial Model)	Error $\lvert\Delta\rvert$	Percentage Error $\frac{\lvert\Delta\rvert}{F_t}\cdot 100\%$	Average Error $\sum\frac{\lvert\Delta_i\rvert}{n}$	Percentage Average Error $\sum\frac{\lvert\Delta_i\rvert}{F_t n}*100\%$
0.9	0.02	55.135	58.015	2.880	5.224	2.306	3.770	57.670	2.535	4.598	2.424	3.922
1.0		57.044	60.118	3.074	5.389			59.913	2.869	5.030		
1.2		62.764	63.940	1.176	1.873			64.003	1.239	1.975		
1.3		63.557	65.693	2.136	3.361			65.886	2.329	3.664		
1.5		66.745	68.949	2.204	3.302			69.391	2.646	3.964		
1.6		68.105	70.469	2.364	3.471			71.032	2.927	4.298		
0.9	0.03	75.480	76.588	1.108	1.469	1.841	2.132	76.013	0.533	0.706	1.611	1.868
1.0		83.828	79.365	4.463	5.324			78.969	4.859	5.796		
1.2		84.340	84.410	0.070	0.083			84.360	0.020	0.024		
1.3		89.932	86.725	3.207	3.566			86.842	3.090	3.436		
1.5		91.842	91.022	0.820	0.892			91.462	0.380	0.414		
1.6		94.408	93.030	1.378	1.460			93.625	0.783	0.830		
		Total average error:				1.915	3.241	Total average error:			1.885	3.228

Table 3. The values of the tangential component F_t of the grinding force obtained experimentally and calculated based on models.

Input Data		Regression Model						Polynomial Model				
v_w [m/min]	a_e [mm]	Tangential Force F_t [N] (Experiment)	Tangential Force F_t [N] (Regression Model)	Error $\lvert\Delta\rvert$	Percentage Error $\frac{\lvert\Delta\rvert}{F_t}\cdot 100\%$	Average Error $\sum\frac{\lvert\Delta_i\rvert}{n}$	Percentage Average Error $\sum\frac{\lvert\Delta_i\rvert}{F_t n}*100\%$	Tangential Force F_t [N] (Polynomial Model)	Error $\lvert\Delta\rvert$	Percentage Error $\frac{\lvert\Delta\rvert}{F_t}\cdot 100\%$	Average Error $\sum\frac{\lvert\Delta_i\rvert}{n}$	Percentage Average Error $\sum\frac{\lvert\Delta_i\rvert}{F_t n}*100\%$
0.9	0.01	5.280	5.776	0.496	1.311	0.855	2.016	7.069	1.789	4.732	1.112	2.755
1.0		6.476	6.107	0.369	0.940			7.529	1.053	2.681		
1.2		6.719	6.725	0.006	0.015			8.399	1.680	4.260		
1.3		9.026	7.016	2.010	4.740			8.812	0.214	0.505		
1.5		8.587	7.568	1.019	2.218			9.601	1.014	2.207		
1.6		9.060	7.830	1.230	2.872			9.980	0.920	2.149		

Table 3. *Cont.*

Input Data			Regression Model					Polynomial Model				
v_w [m/min]	a_e [mm]	Tangential Force F_t [N] (Experiment)	Tangential Force F_t [N] (Regression Model)	Error $\lvert\Delta\rvert$	Percentage Error $\frac{\lvert\Delta\rvert}{F_t} \cdot 100\%$	Average Error $\sum \frac{\lvert\Delta_i\rvert}{n}$	Percentage Average Error $\sum \frac{\lvert\Delta_i\rvert}{F_t n} * 100\%$	Tangential Force F_t [N] (Polynomial Model)	Error $\lvert\Delta\rvert$	Percentage Error $\frac{\lvert\Delta\rvert}{F_t} \cdot 100\%$	Average Error $\sum \frac{\lvert\Delta_i\rvert}{n}$	Percentage Average Error $\sum \frac{\lvert\Delta_i\rvert}{F_t n} * 100\%$
0.9	0.02	12.501	11.975	0.526	0.954	0.724	1.185	12.305	0.196	0.356	0.628	1.025
1.0		14.272	12.662	1.610	2.823			13.107	1.165	2.042		
1.2		14.013	13.944	0.069	0.111			14.621	0.608	0.969		
1.3		14.053	14.547	0.494	0.777			15.340	1.287	2.025		
1.5		16.572	15.691	0.881	1.320			16.714	0.142	0.213		
1.6		17.001	16.236	0.765	1.124			17.373	0.372	0.547		
0.9	0.03	19.338	18.346	0.992	1.315	0.901	1.025	17.018	2.320	3.074	1.163	1.402
1.0		19.975	19.397	0.578	0.689			18.128	1.847	2.204		
1.2		21.197	21.361	0.164	0.195			20.221	0.976	1.157		
1.3		21.716	22.285	0.569	0.633			21.215	0.501	0.557		
1.5		22.865	24.038	1.173	1.277			23.116	0.251	0.273		
1.6		22.945	24.872	1.927	2.042			24.028	1.083	1.147		
Total average error:						0.827	1.409	Total average error:			0.968	1.727

5. Conclusions

The article presents mathematical models in the form of multiple regression functions and polynomial functions, enabling the calculation of the normal component F_n and the tangential component F_t of the grinding force during the sharpening of the rake surfaces of hob cutters. The models were determined based on the results of experimental studies.

Based on the obtained research results, it can be concluded that:

1. Both the experimental results and the results obtained from the calculations based on the models indicate that as the grinding depth a_e increases, the values of the grinding force components (F_n and F_t) also increase, which was expected. A similar relationship was found when the workpiece speed v_w was increased.
2. In the case of the normal component F_n, the overall percentage average errors for both models remain small, amounting to 3.241% for the regression model and 3.228% for the polynomial model. For the tangential component F_t, the overall percentage average error for both models is small, amounting to 1.409% for the regression model and 1.727% for the polynomial model.
3. The values of both grinding force components calculated based on the mathematical models are consistent with the results obtained from the experiment. In the case of the F_n component, the calculated values in both cases deviate insignificantly from the experimental values, while for the F_t component, the results show a very small relative error despite the irregular course of the experimental results, which should be

considered very satisfactory. Additionally, the high value of the multiple regression coefficient for both models demonstrates compliance with the experimental results.

4. The developed models provide a good basis for analyzing the hob cutter sharpening process with variable grinding parameters, and can also be used in modelling the dynamic grinding process.

Author Contributions: Conceptualization, B.W., W.S. and M.S.; Methodology, B.W., W.S. and M.S.; Software, B.W. and W.S.; Validation, B.W., W.S. and N.K.; Formal analysis, B.W., W.S. and W.P.; Investigation, B.W. and W.S.; Data curation, B.W. and W.S.; Writing—original draft, B.W. and W.S.; Writing—review and editing, B.W., W.S., N.K. and W.P. All authors have read and agreed to the published version of the manuscript.

Funding: This research received no external funding.

Institutional Review Board Statement: Not applicable.

Informed Consent Statement: Not applicable.

Data Availability Statement: Data are contained within the article.

Conflicts of Interest: The authors declare no conflicts of interest.

References

1. Korecki, M.; Wołowiec-Korecka, E. Glenn. Single-piece, high-volume, low-distortion case hardening of gears. *Therm. Process.* **2016**, *9*, 32–39.
2. Stachurski, W.; Sawicki, J.; Wójcik, R.; Nadolny, K. Influence of application of hybrid MQL-CCA method of applying coolant during hob cutter sharpening on cutting blade surface condition. *J. Clean. Prod.* **2018**, *171*, 892–910. [CrossRef]
3. Moderow, R. The right and wrong of modern hob sharpening. *Gear Technol.* **1992**, 34–38.
4. Kruszyński, B.; Wójcik, R. Residual stress in grinding. *J. Mater. Process. Technol.* **2001**, *109*, 254–257. [CrossRef]
5. Malkin, S.; Guo, C. *Grinding Technology: Theory and Applications of Machining with Abrasives*, 2nd ed.; Industrial Press Inc.: New York, NY, USA, 2008.
6. Stachurski, W.; Nadolny, K. Influence of the condition of the surface layer of a hob cutter sharpened using the MQL-CCA hybrid method of coolant provision on its operational wear. *Int. J. Adv. Manuf. Technol.* **2018**, *98*, 2185–2200. [CrossRef]
7. Rowe, W.B. *Principles of Modern Grinding Technology*, 2nd ed.; Elsevier: Amsterdam, The Netherlands, 2014.
8. Stachurski, W.; Dębkowski, R.; Rosik, R.; Święcik, R.; Pawłowski, W. Evaluation of the influence of the cooling method used during grinding on the operating properties of ceramic grinding wheels made with different abrasives. *Adv. Sci. Technol. Res. J.* **2023**, *17*, 1–18. [CrossRef]
9. Li, L.; Zhang, Y.; Cui, X.; Said, Z.; Sharma, S.; Liu, M.; Gao, T.; Zhou, Z.; Wang, X.; Li, C. Mechanical behavior and modeling of grinding force: A comparative analysis. *J. Manuf. Process.* **2023**, *102*, 921–954. [CrossRef]
10. Li, B.; Li, X.; Hou, S.; Yang, S.; Li, Z.; Qian, J.; He, Z. Prediction and analysis of grinding force on grinding heads based on grain measurement statistics and single-grain grinding simulation. *Int. J. Adv. Manuf. Technol.* **2024**, *132*, 513–532. [CrossRef]
11. Wang, X.; Liu, Q.Y.; Zheng, Y.; Xing, W.; Wang, M. A grinding force prediction model with random distribution of abrasive grains: Considering material removal and undeformed chips. *Int. J. Adv. Manuf. Technol.* **2022**, *120*, 7219–7233. [CrossRef]
12. Wu, Z.; Zhang, L. Analytical grinding force prediction with random abrasive grains of grinding wheels. *Int. J. Mech. Sci.* **2023**, *250*, 108310. [CrossRef]
13. Yan, Y.; Xu, J.; Wiercigroch, M. Non-linear analysis and quench control of chatter in a plunge grinding. *Int. J. Non-Linear Mech.* **2015**, *70*, 134–144. [CrossRef]
14. Yan, Y.; Xu, J.; Wiercigroch, M. Regenerative chatter in self-interrupted plunge grinding. *Meccanica* **2016**, *51*, 3185–3202. [CrossRef]
15. Yan, Y.; Xu, J.; Wiercigroch, M. Regenerative chatter in a plunge grinding process with workpiece imbalance. *Int. J. Adv. Manuf. Technol.* **2017**, *89*, 2845–2862. [CrossRef]
16. Yan, Y.; Xu, J.; Wiercigroch, M. Chatter in a transverse grinding process. *J. Sound Vib.* **2014**, *333*, 937–953. [CrossRef]
17. Sun, C.; Deng, Y.; Lan, D.; Xiu, S. Modeling and predicting ground surface topography on grinding chatter. *Procedia CIRP* **2018**, *71*, 364–369. [CrossRef]
18. Werner, G. Influence of work material on grinding forces. *Ann. CIRP* **1978**, *27*, 243–248.
19. Meng, Q.; Guo, B.; Zhao, Q.; Li, H.N.; Jackson, M.J.; Linke, B.S.; Luo, X. Modelling of grinding mechanics: A review. *Chin. J. Aeronaut.* **2022**, *36*, 25–39. [CrossRef]

20. Mishra, V.K.; Salonitis, K. Empirical estimation of grinding specific forces and energy based on a modified Werner grinding model. *Procedia CIRP* **2013**, *8*, 287–292. [CrossRef]
21. Cieciura, M.; Zacharski, J. *Probabilistic Methods in Practice*; Vizja Press & IT: Warsaw, Poland, 2007.
22. Kruszyński, B.; Midera, S.; Kaczmarek, J. Forces in generating gear grinding-theoretical and experimental approach. *CIRP Ann.–Manuf. Technol.* **1998**, *47*, 287–290. [CrossRef]
23. Stachurski, W.; Midera, S.; Kruszyński, B. Mathematical model describing the course of the process of wear of a hob cutter for various methods of cutting fluid supply. *Eksploat. Niezawodn.* **2016**, *18*, 123–127. [CrossRef]
24. Stachurski, W.; Sawicki, J.; Krupanek, K.; Midera, S. Mathematical model for determining the expenditure of cooling and lubricating fluid reaching directly the grinding zone. *Arch. Mater. Sci. Eng.* **2018**, *94*, 27–34. [CrossRef]
25. Korzyński, M. *Methodology of the Experiment-Planning, Implementation and Statistical Analysis of the Results of Technological Experiments*; WNT: Warsaw, Poland, 2013.

Disclaimer/Publisher's Note: The statements, opinions and data contained in all publications are solely those of the individual author(s) and contributor(s) and not of MDPI and/or the editor(s). MDPI and/or the editor(s) disclaim responsibility for any injury to people or property resulting from any ideas, methods, instructions or products referred to in the content.